

π -Delocalization in the vicinal lone pairs of hydrazines: Electronic effects in derivatives of 1-(2-nitrophenyl)-1-phenylhydrazine



Joël Poisson, Ian S. Butler, D. Scott Bohle*

Department of Chemistry, McGill University, 801 Sherbrooke Street West, Montréal, QC, H3A 0B8, Canada

ARTICLE INFO

Article history:

Received 23 September 2015

Received in revised form

15 February 2016

Accepted 16 February 2016

Available online 23 February 2016

Keywords:

Nitrogen chemistry

Hydrazines

Stereochemistry

ABSTRACT

Several highly colored, crystalline derivatives of 1-(2-nitrophenyl)-1-phenylhydrazine have been synthesized and characterized by UV–Vis, ^1H - and ^{13}C -NMR, mass and IR spectroscopic methods, as well as by single-crystal X-ray diffraction and combustion elemental analysis. The study indicates that the electronic dependence of one nitrogen atom on the other in these systems becomes more pronounced with a decrease in the difference of their formal hybridization. While 1,1-di-aromatic substitution leads to a formal sp^2 hybridization at one nitrogen atom, introduction of a π -bond in the form of a Schiff base or an acetamide function at the second nitrogen atom leads to different hydrazine conformations and N–N bond lengths. One interpretation of these results is that, in many cases, a greater contribution from σ -bonding from two sp^2 hybridized nitrogen atoms leads to stronger and shorter N–N bonds than do the often proposed N–N π -bonding double bonds in the absence of significant intermolecular forces.

© 2016 Elsevier B.V. All rights reserved.

1. Introduction

One of the stronger contrasts in the chemistry of carbon and nitrogen are the ranges of their single bond lengths. While crystallographically determined C–C single bonds span a relatively narrow range with a medium value of 1.5595(70) Å, single N–N bonds vary markedly with a mean value of 1.3845(0.034) Å and may range up to 2.1 Å [1]. Not too surprisingly, the bond enthalpies for these bonds reflect these trends with, for example, N–N single bonds that are found in remarkably stable heterocycles as well as in weak Van der Waals adducts such as $[\text{NO}]_2$ or in the hydrazines. Related trends are also behind the outstanding synthetic utility of hydrazine derivatives which stems in part from the presence of a responsive N–N bond and the nucleophilicity of the lone pairs of electrons on the nitrogen atoms, which are alpha to one another. While hydrazine itself has a long N–N bond that readily undergoes homolysis, upon derivatization the N–N bond is often retained as a strong, short bond in its products. The conformational consequences of these vicinal lone pairs have been studied extensively in alkyl hydrazines and the increased nucleophilicity of these nitrogen atoms is recognized in the alpha kinetic effect [2]. A particularly striking feature of hydrazine derivatives, however, is the tuneable

nature of these vicinal lone-pair interactions, where not only is the reactivity modified, but the N–N bonding can be converted to double or even robust strong N–N single bonds. Consequently, the alpha-effect has been shown [3] to fall off rapidly in substituted hydrazine derivatives, being dramatically reduced in CH_3NHNH_2 and absent in $(\text{CH}_3)_2\text{NNH}_2$. This variability offers considerable scope for these compounds in analytical [4], electronic [5], optical [6–8], and material applications [9–11]. In contrast, N,N-diaryl hydrazines, Ar_2NNH_2 , generally contain planar and formally sp^2 -hybridized Ar_2N units where the nitrogen lone pair is conjugated with the aromatic rings. In this case lone-pair lone-pair interactions are varied and often weaker.

Recently, we reported a method for the facile preparation of N,N-diaryl hydrazines containing electron-withdrawing substituents [12], which allowed us to prepare a series of related derivatives in order to tune the electronic structure of the N–N bonded framework. Such substitutions illustrate the competition of intramolecular π -bonding to form either an N=N double bond, or, by conjugation through a proximal electron-withdrawing group such as $o\text{-C}_6\text{H}_4(\text{NO}_2)$, a C=N bond. In addition, the possibility of intermolecular interactions, such as London forces and donor-acceptor pairings, may further split or modulate these interactions which gives rise to varying N–N bond strengths. Herein, we describe (1) the effect of substitution with electron donor- or withdrawing organic functional groups on bond order throughout the diaryl and –amino domains of N,N-diarylhydrazines; (2) the

* Corresponding author.

E-mail address: scott.bohle@mcgill.ca (D.S. Bohle).

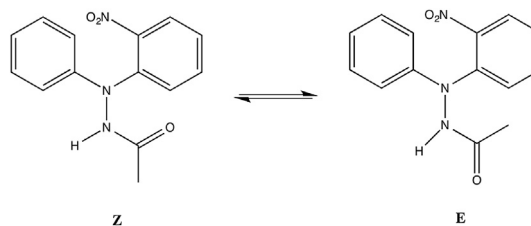
effect on molecular geometry and hence electron mobility across the N–N bond and consequently, the type of N–N bond; (3) the electronic spectroscopy of the new compounds; and (4) the overall implications of these results in terms of molecular stabilities of the hydrazines.

2. Results and discussion

To explore the electronic effects of various substituents in 1,1-diarylhydrazines, 1-(2-nitrophenyl)-1-phenyl hydrazine (NDPH) was derivatized with five different functional groups (Scheme 1). With the exception of the known mono-acetyl derivative **1** all of these compounds are described here for the first time as single well-defined stereoisomers.

The mono-acetylation of NDPH with acetic anhydride results in an equilibrium mixture of isomers for **1**. These correspond to the E and Z isomers around the amide bond, Scheme 2. By ^1H NMR in DMSO there is a 10:1 mixture of Z:E and in chloroform this reaches a more closely balanced 2:1 mixture. Although prior studies [13] have reported similar isomeric ratios in DMSO, we have employed 2D-NOESY NMR to definitively show that in either solution.

The Z isomer is the major species due to the NOE correlation between the more abundant amide proton with the signal for the corresponding acetyl methyl protons (See ESI). These protons give the only significant cross peak in the NOESY spectrum S12, and it suggests that the orthogonal aryl rings result in large inter proton separations for the aryl groups. Given the sharpness of the acetyl peaks in the room temperature ^1H NMR spectrum there is little indication of exchange on the NMR timescale, but this isomerism in amides has been studied mechanistically [14], theoretically using MO theory [15], and has been a subject of considerable biological interest [16–18]. The studies show the Z/E equilibrium to be directly affected by the molecular environment. In the solid state the single crystal X-ray diffraction structure of **1** corresponds solely to the Z isomer, Fig. 1, but when these single crystals are



Scheme 2. Isomerism in N'-(2-nitrophenyl)-N'-phenylacetohydrazide.

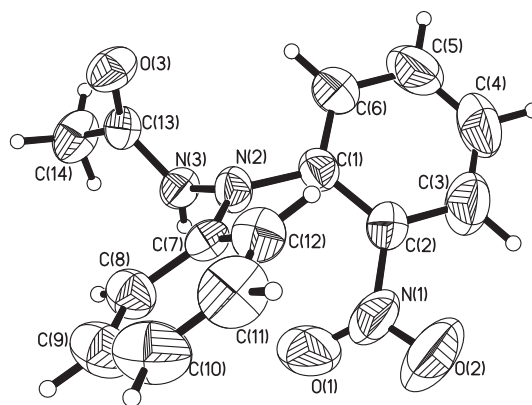
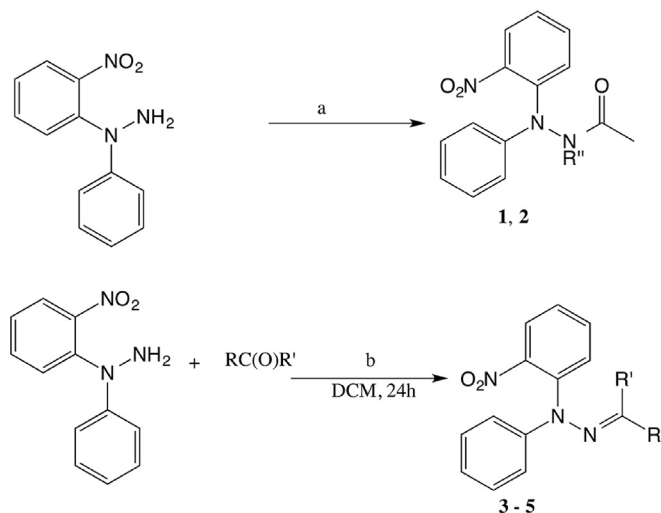


Figure 1. ORTEP representation of one molecule in the asymmetric unit of compound 1. Selected structural parameters are: N(2)–N(3) 1.386(3) Å, N(2)–C(1)–C(2)–N(1) 5.2(5), N(2)–N(3)–C(13)–C(14) –179.9(2).

redissolved, and its NMR spectrum monitored, we find that within mixing/dissolution the same ratio of Z:E isomers in solution is rapidly formed from the single isomer present in the crystal. Gas-phase DFT calculations, B3LYP/6-311++g** (ESI), indicate that the Z isomer has a larger electronic stabilization, some 1.62 kcal/mol more stable than the E isomer, and thus under the conditions of our NMR measurements this would correspond to a 15.3:1 ratio. Solvent polarity and hydrogen bonding ability will clearly alter the position of this equilibrium, and we note that the solid-state structure has intermolecular H-bonding between the amides of neighboring molecules (SI).

Each derivative **1–5** has been characterized by single crystal X-



	1	2	3	4	5
R	H	OAc	Me	H	H
R'	OAc	OAc	Me	o-(C ₆ H ₄)OH	Ph
a	CH ₃ COOH reflux/24 h	3 eq. Ac ₂ O reflux/24 h			
b			H ₂ SO ₄ (cat.)	HCl (cat.)	HCl (cat.)

Scheme 1. Synthesis of 1,1-diarylhydrazine derivatives.

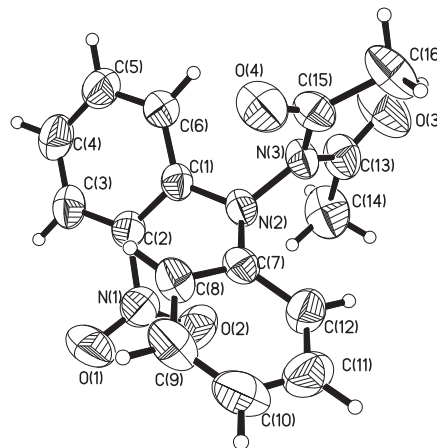


Figure 2. ORTEP representation of compound 2. Selected structural parameters are: N(2)–N(3) 1.402(2) Å, N(2)–C(1)–C(2)–N(1) –0.8(3), O(3)–C(13)–N(3)–N(2) 167.2(2), O(4)–C(15)–N(3)–N(2) –12.8(3), out-of-plane distance of N(3) 0.02(3) Å.

ray diffraction, Figs. 1–5, and the key metric parameters are collected in Table 1. The compounds provide for a different degree of possible electron delocalization and hence deactivation of the remaining nitrogen lone pair from the hydrazine framework. The electronic modulation by the hydrazine substitution has direct consequences on the solid-state structures. Specifically, there are three structural aspects of interest which are directly affected by the electronic properties of the substituent on N(3): (1) the N–N bond length; (2) the orientation of the N-substituents relative to one another; and (3) the formal hybridization state of the nitrogen atoms. For the final consideration, the five derivatives 1–5 were selected because they all share a formally sp^2 hybridized N atom bound to an Ar_2N nitrogen atom. In spite of this similarity, the five derivatives have different N–CR₂ orientations with 1, 2 and 3 having an orthogonal N–CR₂ group to the Ar_2N plane and 4 and 5 having all N substituents coplanar. Although 1, 2, 4 and 5 all have short N–N bonds, there is a significant increase in the N–N bond length upon substitution with an electron-rich 2-propanyl group, =CMe₂, from 1.4159(18) Å in the parent hydrazine to 1.4400(16) Å in 3. Clearly, there is subtle electronic control of this bonding.

Given that substitution with one acetyl group causes such a structural alteration in both the Ar_2N and NH_2 moieties of NDPH, we prepared the diacetyl derivative 2 for comparison. As found for 1 the N(C(O)Me)₂ group in 2 is planar and orthogonal to the Ar_2N group. However the N–N bond in 2 is slightly longer than for that found in 1. Structural studies on di-acetylated hydrazine derivatives are sparse with only 8 structures having been described (Table S1) [19–26]. As can be seen from Table S1, most of the structurally characterized N,N-diacetylhydrazines contain a short N–N bond and a roughly planar sp^2 -hybridized N(C(O)Me)₂ nitrogen. Substitution of the adjacent nitrogen with bulky electron-withdrawing phenyl rings as in 2 (Fig. 2) produces an unusual structural effect that is present in only a couple entries in Table 2. It contains a rather long N–N bond, similar to that seen in the structures of 2,3,4-tri-O-acetyl-N-(diacetylamino)- β -D-glucopyranurono-1,6-lactam reported by Akimoto [21] and N,N'-Diacetyl-N'-(4-nitrophenoxy)acetyl]acetohydrazide, which was reported by Hu [22]. A common feature of both structures is their electron-withdrawing carbonyl functionalities flanking both sides of the N–N bond. As with 2 these structures also have both nitrogen atoms in sp^2 -hybridization states.

Condensation of NDPH with acetone leads to 3 with an electron-rich 2-propanylimine group (Fig. 3) which has the longest N–N σ -bond of all the derivatives examined here. With a torsion angle

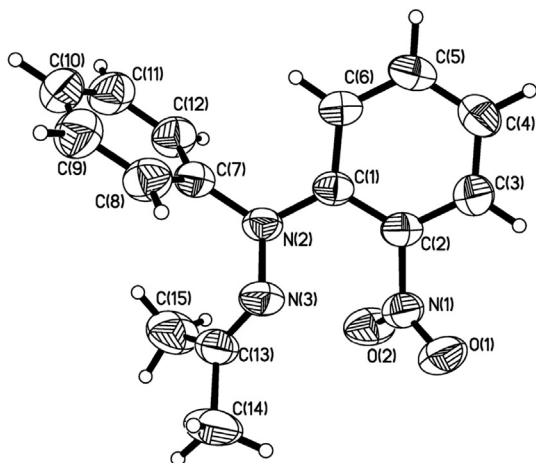


Figure 3. ORTEP Representation of Compound 3. Selected structural parameters are: N(2)–N(3) 1.4400(16) Å, N(2)–C(1)–C(2)–N(1) 8.7(2), N(2)–N(3)–C(13)–C(14) –178.4(1).

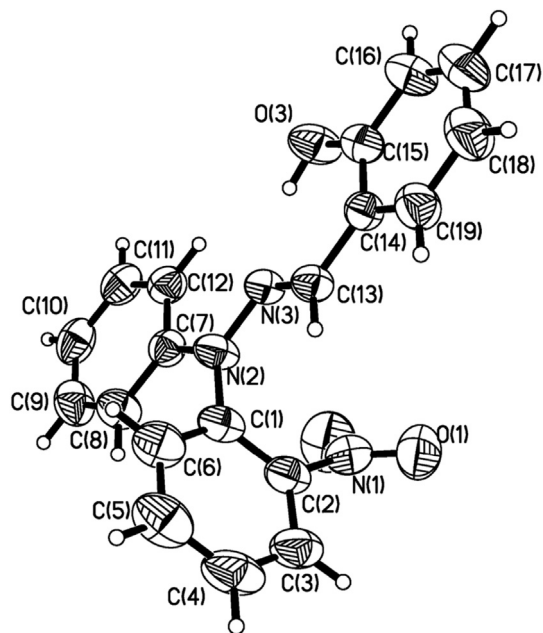


Figure 4. ORTEP Representation of 4. Selected structural parameters are: N(2)–N(3) 1.386(3) Å, N(2)–C(1)–C(2)–N(1) 5.2(5), N(2)–N(3)–C(13)–C(14) –179.9(2).

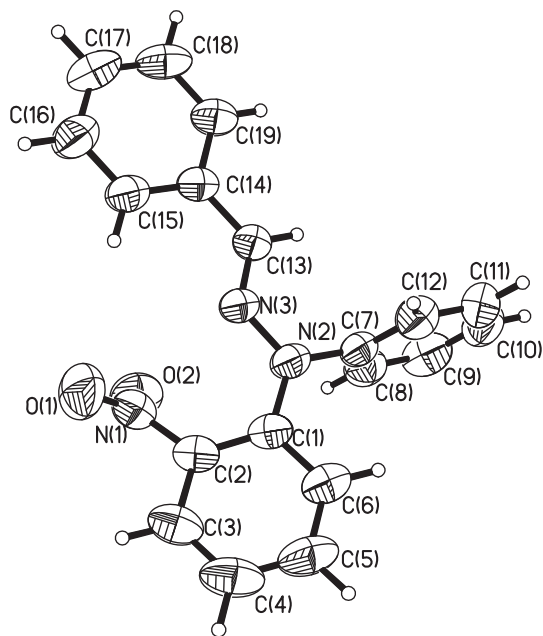


Figure 5. ORTEP Representation of 5. Selected structural parameters are: N(2)–N(3) 1.369(2) Å, N(2)–C(1)–C(2)–N(1) 5.2(5), N(2)–N(3)–C(13)–C(14) –179.9(2)

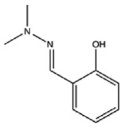
around N(2)–C(1) of 36.68(12), very little π -delocalization of the added electron density on N(3) is possible, but there is nevertheless a shorter N(2)–C(1) bond than in NDPH. The other phenyl ring, in contrast, is orthogonal to the N–N bond as well as the $C_6H_4NO_2$ ring and has a longer N(2)–C(7) bond. As a result of these geometric considerations, the diarylamino nitrogen N(2) is forced out of the plane of its surrounding functional groups by a distance of 0.321 Å, further hindering π -based delocalization.

Schiff base formation by condensation of NDPH with benzaldehyde and salicylaldehyde gives 4 and 5 respectively. By single crystal X-ray diffraction they have the shortest N–N bonds of the

Table 1
X-ray diffraction structural parameters for derivatives of 1-(2-nitrophenyl)-1-phenylhydrazine.

Parameter	NDPH [3]	1	2	3	4	5
N(2)–N(3) (Å)	1.4159 (18)	1.386 (3)	1.402 (2)	1.4400 (16)	1.3748 (13)	1.369 (2)
N(2)–C(1) (Å)	1.4012 (17)	1.409 (4)	1.411 (2)	1.3994 (18)	1.4246 (14)	1.391 (2)
N(2)–C(7) (Å)	1.4134 (18)	1.409 (4)	1.423 (2)	1.4362 (19)	1.4064 (15)	1.424 (2)
N(3)–C(13) (Å)	N/A	1.343 (3)	1.406 (3)	1.273 (2)	1.2845 (14)	1.272 (2)
C(1)–C(2) (Å)	1.3981 (19)	1.381 (4)	1.395 (3)	1.399 (2)	1.3862 (18)	1.382 (2)
C(2)–N(1) (Å)	1.4624 (19)	1.469 (4)	1.468 (3)	1.4703 (18)	1.4590 (18)	1.461 (2)
C(13)–N(3)–N(2)–C(1) (°)	N/A	110.03 (30)	–83.0 (2)	–151.09 (11)	–6.88 (16)	–178.0 (1)
C(13)–N(3)–N(2)–C(7) (°)	N/A	191.68 (30)	121.7 (2)	70.17 (12)	176.39 (10)	4.3 (2)
N(3)–N(2)–C(1)–C(2) (°)	–41.63	–115.97 (30)	154.8 (2)	36.68 (12)	–72.07 (15)	24.2 (2)
N(3)–N(2)–C(7)–C(8) (°)	–163.49	–6.7 (3)	130.4 (2)	–146.23 (12)	–179.24 (11)	–99.7 (2)
N(2)–N(3)–C(13)–C(14) (°)	N/A	–179.9 (2)	–11.7 (3)	–178.44 (12)	–177.55 (10)	178.3 (1)
C(1)–N(2)–N(3) (°)	113.69 (11)	114.0 (2)	116.76 (15)	111.33 (11)	120.72 (9)	115.7 (1)
C(7)–N(2)–N(3) (°)	120.64 (11)	117.6 (2)	116.09 (14)	115.36 (11)	117.89 (9)	122.6 (1)
C(7)–N(2)–C(1) (°)	123.66 (12)	124.4 (2)	122.02 (14)	118.49 (11)	121.31 (9)	121.7 (1)
Sum of angles about N(2) (°)	357.99 (20)	356.0 (3)	354.87 (25)	345.18 (19)	359.92 (16)	360.0 (2)
Distance of N(2) from its plane (Å)	0.1158	0.164 or 0.051 ^a	0.186	0.321	0.023	0.016 or 0.018 ^a

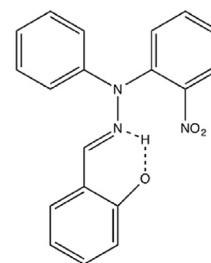
^a Two independent molecules per asymmetric unit.**Table 2**
Comparison of bond lengths in dimethyl- and (Diarylhydrazono)methylphenol derivatives.

Bond	Bond length in compound 4 (Å)	Analogous calculated bond lengths in	
			
		(MINDO) [28]	
		B3LYP/6-311++g**	
O(3)–C(15)	1.359 (2)	1.372	1.35022
C(15)–C(14)	1.401 (1)	1.400	1.41761
C(14)–C(13)	1.452 (2)	1.464	1.45833
C(13)–N(3)	1.284 (2)	1.289	1.29236
N(3)–N(2)	1.375 (1)	1.385	1.36289
N(3)–O(3)	2.650 (1)		2.66002

derivatives studied here. This observation is interestingly in line with pre-quantum mechanical assertions made in 1913 by Graziani [27]. The experimental values obtained here can also be compared with the semiempirical SCF-MO calculations performed by Bren and co-workers for (*E*)-2-((2,2-dimethylhydrazono)methyl)phenol (Table 2) [28], which illustrate the added stability of **4** over its dimethyl analog.

In addition, a small increase in planarity as compared to compound **1** is seen in the solid state (Fig. 4) with N(2) being only 0.023 Å out of the plane of its substituents. The phenolic proton of the salicylaldehyde group forms an internal hydrogen bonding (O(3)–N(3) = 2.650(1) Å) and hence only the *E*-isomer is observed in the solid state and in solution. This is seen as a broadening and downfield shift of the O–H signal in the NMR, from that of salicylaldehyde [29], as well as in the considerable broadening of the $\nu(\text{OH})$ in the IR spectrum.

The bond lengths for **4** are commensurate with or even shorter than those predicted theoretically [28] by semiempirical MINDO methods for the dimethyl analog. Allowing for decreased steric hindrance and increased planarity, this particular derivative is perfectly engineered to efficiently delocalize electron density throughout the entire molecule and form a stable $\text{sp}^2\text{-sp}^2$ N–N bond. In addition, the salicylaldehyde adducts are stabilized by intramolecular hydrogen bonding (Fig. 6), with an O(3)–N(3) distance of 2.650(1) Å.

**Figure 6.** Intramolecular hydrogen bonding in **4**.

To definitively examine the role of hydrogen bonding in the decreased N–N bond length in **4** and in 1,1-diaryl hydrazines, the adduct of NDPH and benzaldehyde (**5**) was synthesized from NDPH and structurally characterized (Fig. 5). The reverse reaction, the hydrolysis of **5** to give NDPH, is known in the literature prior to our work [13] but it has not been structurally characterized.

Although **5** cannot form a stabilizing hydrogen bond, its hydrazine/Schiff's base geometry is isostructural with **4**. With a distance of 0.016 Å separating N(2) from the plane formed by its substituents, this derivative is the most planar at nitrogen N(2), suggesting pronounced sp^2 -hybridization at its diaryl nitrogen. In addition, the N–N bond and the ortho-nitro substituent are coplanar, with the latter feature being unique amongst the five structures **1–5**.

In order to interpret any of the structural data for the Ar_2N moiety we sought to establish the presence and/or absence of significant intermolecular π -stacking interactions. In Fig. 7 the variation of N–N bond lengths is plotted against the N(2)–C(1) and N(2)–C(7) bond lengths, as well as the sum of their lengths. In addition, the closest intermolecular approaches in the solid state are listed in Table 3. Critically in none of these structures do the aromatic rings orient and pack in ways that would lead to significant π - π stacking interactions. Packing in these structures is dominated by off set edge “herringbone” side on interactions.

To assess any significant donor-acceptor interactions, the UV–visible spectra of the compounds in chloroform were acquired and the lowest energy transitions were tabulated (Table 4). Two aspects of molar absorptivity and absorption maxima for **1–5**, warrant discussion. First is the apparent spread of the peak absorption values. There is a red shift of the $n \rightarrow \pi^*$ transition in the order **5** < **4** < **2** < **3** < **1** with the position of **4** relying on the presence of its phenolic proton. This trend is in line with structural aspects of

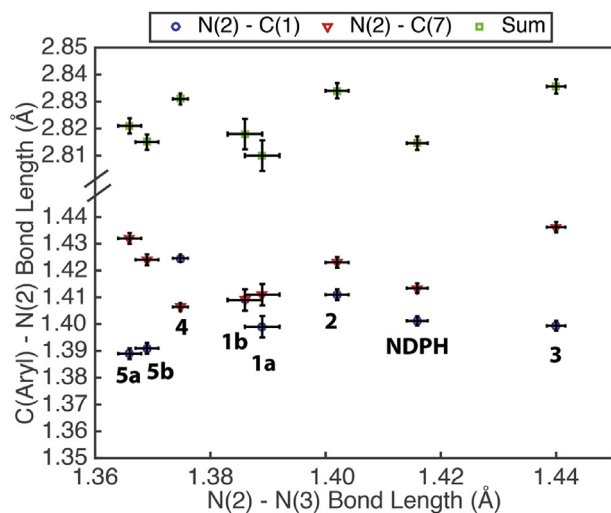


Figure 7. Variation in C–N bond length with N–N separation. Suffixes (a, b) denote independent molecules in the unit cells of 1 and 5.

these derivatives. With the exception of **4** the extinction coefficients are all similar and consistent with $n - \pi^*$ transitions. In compound **4** this band is overlapped by an intense $\pi - \pi^*$ transition, which possibly owes its lower energy to the stabilizing effects of the internal hydrogen bonding and extensive conjugation in that derivative.

A general trend operating in these systems is a direct correlation between the C(7)–N(2) bond length which is slightly longer than the C(1)–N(2) bond lengths and this difference is accentuated for the longer and shorter N(2)–N(3) bond lengths. These bond lengths reflect aryl competition for N(2) π -bonding, but their sum remains fairly constant, 2.825(0.01) Å.

One of the most interesting aspects of the bonding in **1–5** is the possibility of N–N bond contraction from either π – bond formation or from valence re-hybridization as sp^2 – sp^2 single bonds. Both would be expected to lead to N–N bond shortening and planar nitrogen (Table 1). However types **2a** and **2b** will differ in that π – bond formation requires coplanarity of the Ar_2N and NR_2 fragments to ensure p–p overlap at the nitrogen atoms. Table 5 describes aspects of this formal view, with **1–5** falling under categories **2a** and **b** and ranking $5 < 4 < 1 < 2 < NDPH < 3$ in terms of N–N bond length.

3. Conclusions

From 1-(2-nitrophenyl)-1-phenyl hydrazine, synthesized under oxidative conditions, several derivatives can be made in good yield and of high purity. These derivatives illustrate the electronic interplay between the diaryl system and any substituents on the terminal NH_2 group of the parent hydrazine, which are nearly unaffected by intermolecular interactions as demonstrated by UV–visible data. The effects of these two environments can work

Table 4
Lowest energy UV–Visible absorption bands for NDPH derivatives.

Compound	λ_{max} (nm)	Molar absorbance (ϵ) $M^{-1} cm^{-1}$
1	418	1540
2	377	2950
3	410	3680
4	338	20500
5	324	1340

synergistically by reducing the N–N repulsion between the nitrogen lone pairs, providing an even more stable N–N bond; or antagonistically, should the electronic environments of the N–N nitrogen atoms become congruent and lone pair repulsion be increased.

The balance of the electronic environments in these hydrazines can be quantified in the solid-state by measuring the N–N bond length. This bond length can vary from a long N–N bond typical of hydrazine itself, which is rather reactive to a length reminiscent of a double bond. Surprisingly, the structural orientations reported here, supported by DFT calculations, suggest that the π -contribution to the short bond distances is minimal. This suggests overwhelming σ -bonding effects, which are strengthened in systems where the nitrogen atoms are made electronically dissimilar, whereas similar electronic environments for both nitrogen atoms, even equivalent π -delocalization of the N-lone pairs, results in repulsion, decreased σ -overlap and a longer N–N bond. This knowledge is useful for the production of stable hydrazine derivatives as potential reagents in organic synthesis and analytical studies.

4. Experimental

4.1. General methods

Dichloromethane was continuously dried over a column of SiO_2 . All other reagents and solvents were obtained from commercial sources and were used as received. 1H and ^{13}C -NMR spectra were recorded on 300 and 500 MHz Varian spectrometers. High-resolution mass spectra (HRMS) was measured by electrospray techniques with a time-of-flight detector (ESI/TOF). UV/Vis spectra of all the compounds were acquired on a Carey 100 Bio spectrophotometer. Melting and decomposition points were determined using a TA Instruments DSC (Manufacturer?) with samples sealed in aluminum pans under a nitrogen atmosphere, using heating rates of 2 °C/min to within 10 °C of the melting temperature determined by a micromelting apparatus and then slowed 0.5 °C/min.

4.1.1. *N'*-(2-nitrophenyl)-*N'*-phenylacetohydrazide (**1**)

1-(2-nitrophenyl)-1-phenylhydrazine (0.3000 g, 1.31 mmol) was dissolved in concentrated acetic acid (15 mL) under $N_2(g)$ and the solution was heated at reflux overnight. After cooling to room temperature, the solution was neutralized with aqueous sodium

Table 3
Closest intermolecular interactions in NDPH derivatives.

Compound	Ph	Ph(NO_2)	$R_{N(3)}$
1	3.666 Å (C(20)–C(6))	3.213 Å (C(4)–O(5))	3.527 (C(28)–O(3))
2	3.701(3) Å (C(10)–C(16))	3.761(3) Å (C(3)–C(12))	3.199(3) (C(4)–O(4))
3	3.767(3) (C(9)–C(5))	3.878(2) Å (O(2)–C(14))	3.878(2) Å (O(2)–C(14))
4	3.8311(2) (C(3)–C(10))	3.539(2) Å (C(4)–O(1))	3.562(1) Å (C(13)–O(3))
5	3.068 (O(1)–C(32))	3.068 (O(1)–C(32))	3.570(3) Å (C(18)–C(25))

Table 5
Formal description of bonding in Ar₂NNR₂.

Type	N Hybridization states	Geometry	Relative bond strength	Contributing bonding interactions
1	sp ² -sp ³		Weak	σ only
2a	sp ² -sp ² (available lone pairs)	orthogonal	Strong	σ only
2b	sp ² -sp ² (delocalized lone pairs)	coplanar	Strong	σ and π
3	sp ² -sp ² (no available lone pairs)		Strong	σ only

bicarbonate (5% w/w) and then extracted (3 × 20 mL) with ether. The organic washings were dried (MgSO₄) and left to crystallize at 0 °C, giving the dark red crystalline product (0.2506 g, 70% yield); m.p. (DSC) onset 141.56 °C (lit. 140.9 °C), peak max 143.30 °C (lit. [13] 141.7 °C); ¹H-NMR (300 MHz, DMSO-d₆) δ (ppm) mixture of *E*- and *Z*-isomers, *Z*-isomer: 1.89 (3H, s), 6.76 (d, 2H, J = 7.80 Hz), 6.90 (1H, t, J = 7.50 Hz), 7.21 (t, 2H, J = 7.80 Hz), 7.35 (1H, t, J = 8.10 Hz), 7.53 (d, 1H, J = 8.10 Hz), 7.67 (t, 1H, J = 8.40 Hz), 7.85 (d, 1H, J = 8.10 Hz), 10.49 (s, 1H); *E*-isomer: 1.94 (3H, s), 6.81 (d, 2H, J = 7.80 Hz), 7.02 (1H, t, J = 7.50 Hz), 7.27 (t, 2H, J = 7.80 Hz), 7.40 (1H, t, J = 8.10 Hz), 7.57 (d, 1H, J = 8.10 Hz), 7.78 (t, 1H, J = 8.40 Hz), 7.92 (d, 1H, J = 8.10 Hz), 10.09 (s, 1H); ¹³C-NMR (300 MHz, DMSO-d₆) δ (ppm), only *Z*-isomer detectable: 20.7, 116.0, 121.9, 125.6, 125.9, 126.9, 129.4, 134.5, 138.6, 146.1, 157.8, 169.5; UV-Vis (CHCl₃): λ_{max} = 418 nm, ε = 1541 M⁻¹ cm⁻¹; HRMS calcd for C₁₄H₁₂N₃O₃: 270.0884, Found: 270.0873; Anal. Calcd for C₁₄H₁₃N₃O₃: C, 61.99%; H, 4.83%; N, 15.49%; Found: C, 61.91%; H, 4.78%; N, 15.59%.

4.1.2. *N*-acetyl-*N'*-(2-nitrophenyl)-*N'*-phenylacetohydrazide (**2**)

1-(2-nitrophenyl)-1-phenylhydrazine (150 mg, 0.65 mmol) was dissolved in chloroform (50 mL) along with 5 mL of acetic anhydride. The reactants were heated at 60 °C for 2 days, at which point TLC (dichloromethane) indicated consumption of the starting material. The solution was reduced *in vacuo* and the residue was dissolved in ethanol (15 mL). After cooling for 24 h at -10 °C, which crystals of **2** began to form. Yield 0.173 g (0.55 mmol, 84% yield). A sample was recrystallized from dichloromethane to yield red prisms. m.p. (DSC) onset 172.05 °C, peak max 173.75 °C; ¹H-NMR (300 MHz, CDCl₃) δ (ppm): 2.52 (6H, s), 6.97 (d, 2H, J = 8.40 Hz), 7.09 (1H, t, J = 7.50 Hz), 7.12 (d, 1H, J = 4.50 Hz), 7.19 (1H, t, H = 7.50 Hz), 7.27 (m, 2H), 7.54 (t, 1H, J = 7.50 Hz), 7.77 (d, 1H, J = 8.10 Hz); ¹³C-NMR (300 MHz, CDCl₃) δ (ppm): 25.6, 118.6, 121.0, 123.7, 125.1, 125.9, 129.5, 129.6, 134.0, 136.9, 144.0, 172.8; IR (KBr, cm⁻¹): 477 (vw), 525 (w), 587 (w), 596 (vw), 631 (m), 665 (vw), 701 (m), 744 (m), 758 (m), 776 (m), 828 (w), 857 (w), 903 (vw), 919 (vw), 938 (vw), 950 (vw), 991 (m), 1028 (vw), 1042 (vw), 1137 (sh), 1165 (w), 1203 (vs), 1234(s), 1261 (w), 1287 (w), 1301 (w), 1321 (vw), 1365 (s), 1415 (w), 1456 (w), 1482 (s), 1491 (s), 1530 (vs), 1597 (m), 1718 (vs), 1734 (vs), 3044 (vw); UV-Vis (CHCl₃): λ_{max} = 445 nm, ε = 1095 M⁻¹ cm⁻¹, λ_{max} = 377 nm, ε = 2952 M⁻¹ cm⁻¹, λ_{max} = 259 nm, ε = 17130 M⁻¹ cm⁻¹; HRMS calcd for C₁₆H₁₅N₃O₄Na: 336.0955, Found: 336.0944; Anal. Calcd for C₁₆H₁₅N₃O₄: C, 61.34%; H, 4.83%; N, 13.41%; Found: C, 61.69%; H, 4.80%; N, 13.48%.

4.1.3. 1-(2-nitrophenyl)-1-phenyl-2-(propan-2-ylidene)hydrazine (**3**)

1-(2-nitrophenyl)-1-phenylhydrazine (0.0853 g, 0.373 mmol) was dissolved in dry dichloromethane (50 mL). HPLC-grade acetone (10 mL) was added, along with a catalytic amount of concentrated sulfuric acid. The reaction was stirred for 15 h at room temperature. Evaporation of the solvents and acid under high vacuum yielded the crude product, which was recrystallized by slow evaporation from dichloromethane to give 0.055 g of an orange crystalline product (0.20 mmol, 54%); m.p. 81.2–82.0 °C; ¹H-NMR (300 MHz, CDCl₃) δ (ppm): 1.80 (s, 3H), 2.10 (s, 3H), 7.09 (m, 5H), 7.31 (tt, 3H),

7.74 (dd, 1H); ¹³C-NMR (300 MHz, CDCl₃) δ (ppm): 21.1, 24.6, 122.3, 122.6, 122.8, 124.3, 125.5, 129.5, 132.5, 142.5, 143.8, 146.1, 173.1; IR (KBr, cm⁻¹): 419 (vw), 428 (vw), 437 (vw), 466 (vw), 497 (vw), 520 (w), 533 (w), 614 (vw), 640 (vw), 678 (vw), 705 (s), 713 (w), 741 (s), 751 (w), 770 (m), 776 (m), 841 (m), 850 (m), 906 (vw), 923 (vw), 942 (vw), 993 (vw), 1004 (vw), 1026 (vw), 1050 (vw), 1072 (w), 1093 (sh), 1156 (w), 1173 (w), 1205 (w), 1255 (m), 1272 (m), 1292 (m), 1309 (sh), 1324 (vw), 1363 (s), 1426 (vw), 1447 (w), 1486 (s), 1524 (vs), 1573 (w), 1591 (m), 1602 (m), 1630 (vw), 1644 (vw), 1955 (vw), 1972 (vw), 2915 (vw), 2951 (vw), 2991 (vw), 3034 (vw), 3064 (vw); UV-Vis (CHCl₃): λ_{max} = 410 nm, ε = 3681⁻¹ cm⁻¹; HRMS calcd for C₁₅H₁₅N₃O₂Na: 292.1056, Found: 292.1052; Anal. Calcd for C₁₅H₁₅N₃O₂: C, 66.90%; H, 5.61%; N, 15.60%; Found: C, 66.62%; H, 5.48%; N, 15.63%.

4.1.4. (*Z*)-2-((2-(2-nitrophenyl)-2-phenylhydrazono)methyl)phenol (**4**)

To a 250 mL round-bottomed flask under N₂ (g) was added a solution of 1-(2-nitrophenyl)-1-phenylhydrazine (0.1700 g, 0.44 mmol) in dry dichloromethane (20 mL) along with 2 drops each of salicylaldehyde and hydrochloric acid. The red reaction mixture was stirred for 12 h at room temperature, during which, the solution adopted a lighter orange color. The product was obtained as a crude solid by simple evaporation of the solvent under reduced pressure and recrystallized from dichloromethane:ethanol (1:2) to give red crystals in 0.2004 g (0.60 mmol, 81%) yield. m.p. (DSC) onset 125.53 °C, peak max 127.06 °C; ¹H-NMR (300 MHz, CDCl₃) δ (ppm): 6.83 (t, 1H, J = 8 Hz), 6.96 (t, 2H, J = 8 Hz), 7.03 (d, 2H, J = 8 Hz), 7.11 (t, 1H, J = 7 Hz), 7.22 (t, 1H, J = 8 Hz), 7.35 (t, 2H, J = 8 Hz), 7.39 (s, 1H), 7.40 (d, 1H, 8 Hz), 7.56 (t, 1H, J = 8 Hz), 7.76 (t, 1H, J = 10 Hz), 8.04 (d, 1H, J = 8 Hz), 10.90 (s, 1H); ¹³C-NMR (300 MHz, CDCl₃) δ (ppm): 116.8, 118.4, 118.8, 119.4, 123.9, 126.1, 128.6, 129.7, 130.2, 130.4, 130.5, 134.5, 134.7, 142.3, 143.7, 147.2, 157.1; IR (KBr, cm⁻¹): 472 (w), 553 (w), 588 (w), 624 (vw), 657 (w), 667 (w), 688 (s), 712 (w), 746 (vs), 759 (s), 776 (w), 795 (w), 810 (vw), 848 (m), 1033 (w), 1071 (w), 1098 (vw), 1153 (w), 1220 (s), 1271 (s), 1296 (m), 1363 (s), 1387 (vw), 1413 (vw), 1496 (vs), 1527 (vs), 1594 (vs), 1620 (w), 2875 (vw), 3042 (vw); UV-Vis (CHCl₃): λ_{max} = 338 nm, ε = 20471 M⁻¹ cm⁻¹; λ_{max} = 241 nm, ε = 170,000 M⁻¹ cm⁻¹; HRMS calcd for C₁₉H₁₅N₃O₃Na: 356.1002, Found: 356.1006; Anal. Calcd for C₁₉H₁₅N₃O₃: C, 68.46%; H, 4.54%; N, 12.61%; Found: C, 68.26%; H, 4.31%; N, 12.43%.

4.1.5. (*E*)-2-Benzylidene-1-(2-nitrophenyl)-1-phenylhydrazine (**5**)

1-(2-nitrophenyl)-1-phenylhydrazine (145 mg, 0.63 mmol) was dissolved in dichloromethane (50 mL) along with benzaldehyde (120 μL, 1.17 mmol) was added along with anhydrous magnesium sulfate (0.23 g, 1.91 mmol). The yellow solution was stirred for 12 h at room temperature. The solvent was removed under reduced pressure and the residue loaded onto a silica gel column with dichloromethane as eluent. The first yellow band was collected and the solvent evaporated to yield the pure product directly as a yellow solid in 0.115 g (0.36 mmol, 57% yield). A sample was recrystallized from dichloromethane to yield yellow prisms. m.p. (DSC) onset 109.22 °C (lit. 102.6 °C), peak max 109.64 °C (lit. [13] 104.8 °C); ¹H-NMR (500 MHz, CDCl₃) δ (ppm): 7.11 (1H, d, J = 8.50 Hz), 7.17 (t, 4H,

$J = 6.0$ Hz), 7.25 (d, 1H, $J = 7.50$ Hz), 7.29–7.34 (m, 3H), 7.38 (t, 2H, $J = 8$ Hz), 7.51 (d, 2H, $J = 7.50$ Hz), 7.55 (d, 1H, $J = 7.50$ Hz), 7.86 (d, 1H, $J = 9$ Hz); ^{13}C -NMR (500-MHz, CDCl_3) δ (ppm): 122.0, 125.0, 125.6, 125.9, 126.6, 127.3, 128.6, 128.7, 129.7, 133.4, 135.1, 136.9, 137.8, 142.8, 145.6; UV–Vis (CHCl_3): $\lambda_{\text{max}} = 324$ nm, $\epsilon = 1341 \text{ M}^{-1} \text{ cm}^{-1}$; HRMS calcd for $\text{C}_{19}\text{H}_{15}\text{N}_3\text{O}_2\text{Na}$: 340.1056, Found: 340.1068; Anal. Calcd for $\text{C}_{19}\text{H}_{15}\text{N}_3\text{O}_2$: C, 71.91; H, 4.76; N, 13.24; Found: C, 71.63; H, 4.66; N, 13.29.

4.2. X-ray crystallography

The X-ray diffraction data were measured with graphite monochromated Mo $K\alpha$ radiation ($\lambda = 0.71073 \text{ \AA}$) on crystals that were attached to a glass fiber with viscous paratone N oil. The structures were solved by direct methods on an absorption-corrected model generated by SADABS. Refinement was achieved by a full-matrix least-squares procedure based on F^2 . The hydrogen atoms were located at calculated positions.

Acknowledgements

This research was supported by NSERC discovery grants to DSB and ISB. The authors are grateful to Dr. Alexander Wahba and Nadim Saade for mass spectrometry analysis.

Appendix A. Supplementary data

Supplementary data related to this article can be found at <http://dx.doi.org/10.1016/j.molstruc.2016.02.061>.

References

- [1] Cambridge Crystallographic Structural Database. CCSD: Cambridge, 2015.
- [2] N.J. Fina, J.O. Edwards, *Int. J. Chem. Kinet.* 5 (1973) 1–26.
- [3] T.C. Bruice, A. Donzel, R.W. Huffman, A.R. Butler, *J. Am. Chem. Soc.* 89 (1967) 2106–2121.
- [4] S.B. Kedare, R.P. Singh, *J. Food. Sci. Technol.* 48 (2011) 412–422.
- [5] (a) J. Koller, H.M. Ajmera, K.A. Abboud, T.J. Anderson, L. McElwee-White, *Inorg. Chem.* 47 (2008) 4457–4462; (b) T.M. Krygowski, B.T. Stepien, *Chem. Rev.* 105 (2005) 3482–3512.
- [6] M.J. Davies, B.C. Gilbert, K.A. McLauchlan, in: *Electron Paramagnetic Resonance; The Royal Society of Chemistry: Cambridge, UK, 2000*, pp. 178–179.
- [7] N. Romanov, C. Anastasi, C. Liu, WO2013041117A1 2013.
- [8] P. Shen, X. Liu, S. Jiang, L. Wang, L. Yi, D. Ye, B. Zhao, S. Tan, *Dyes Pigm.* 92 (2012) 1042–1051.
- [9] D. Demeter, S. Mohamed, A. Diac, I. Grosu, J. Roncali, *ChemSusChem* 7 (2014) 1046–1050.
- [10] M. Yanase, Y. Hara, JP2010176976A 2010.
- [11] I.A. Tonks, A.C. Durrell, H.B. Gray, J.E. Bercaw, *J. Am. Chem. Soc.* 134 (2012) 7301–7304.
- [12] C.D. Bain, J.M. Bayne, D.S. Bohle, I.S. Butler, J. Poisson, *Can. J. Chem.* 92 (2014) 904–912.
- [13] A.A. Berezin, G. Zissimou, C.P. Constantinides, Y. Beldjoudi, J.M. Rawson, P.A. Koutentis, *J. Org. Chem.* 79 (2014) 314–327.
- [14] C. Dugave, *General Mechanisms of Cis-Trans Isomerization: A Rapid Survey*; cis-trans Isomerization in Biochemistry, Wiley-VCH Verlag GmbH & Co. KGaA, 2006, pp. 7–13.
- [15] P.R. Andrews, *Biopolymers* 10 (1971) 2253–2267.
- [16] J.-C. Micheau, J. Zhao, *J. Phys. Org. Chem.* 20 (2007) 810–820.
- [17] C. Schiene-Fischer, C. Luecke, *Secondary Amide Peptide Bond Cis/Trans Isomerization in Polypeptide Backbone Restructuring: Implications for Catalysis*, Protein Folding Handbook, 2005, pp. 415–428.
- [18] C. Dugave, L. Demange, *Chem. Rev. Wash. DC U. S. A.* 103 (2003) 2475–2532.
- [19] M.E. Derieg, J.F. Blount, R.I. Fryer, S.S. Hillery, *Tetrahedron Lett.* 11 (1970) 3869–3872.
- [20] C.-L. He, Z.-M. Du, Z.-Q. Tang, X.-M. Cong, L.-Q. Meng, *Acta Crystallogr. Sect. E* 65 (2009) o1902.
- [21] T. Akimoto, Y. Takeda, Y. Nawata, Y. Iitaka, *Acta Crystallogr. Sect. C* 44 (1988) 760–762.
- [22] X. Hu, Z. Wang, W. Xu, G. Zhao, R. Wang, *Acta Crystallogr. Sect. E* 65 (2009) o372.
- [23] I. Wolska, E. Hejchman, *Acta Crystallogr. Sect. E* 59 (2003) o2007–o2009.
- [24] D. Sun, M. Krawiec, C.F. Campana, W.H. Watson, *J. Chem. Crystallogr.* 27 (1997) 577–588.
- [25] R. Nakahara, M. Doi, Y. Kitani, T. Yamaguchi, Y. Fujita, *X-ray Struct. Anal. Online* 25 (2009) 21–22.
- [26] M. Struga, J. Kossakowski, B. Mirosław, A.E. Koziol, *Molbank* (2007) M533.
- [27] F. Graziani, F. Bovini, *Atti. Accad. Naz. Lincei. Cl. Sci. Fis. Mat. Nat. Rend.* 22 (1913) 793–797.
- [28] V.A. Bren, T.M. Stul'neva, B.Y. Simkin, V.I. Minkin, *Zh. Org. Khim.* 12 (1976) 633–640.
- [29] R.J. Abraham, M. Mobli, R.J. Smith, *Magn. Reson. Chem.* 41 (2003) 26–36.